Proceedings of the 9th International Conference on Fluid Flow, Heat and Mass Transfer (FFHMT'22)
Niagara Falls, Canada – June 08-10, 2022
Paper No. 151
DOI: 10.11159/ffhmt22.151

HEAT TRANSFER ANALYSIS OF THE SPIRAL BAFFLED JACKETED MULTIPHASE OXYGEN REACTOR IN THE HYDROGEN PRODUCTION Cu-Cl CYCLE

Mohammed W. Abdulrahman
Rochester Institute of Technology
mwacad@rit.edu

Abstract **-** In this paper, the heat transfer analysis of the three-phase oxygen reactor with a spiral baffled jacketed reactor are performed. The required number of oxygen reactors is analysed to provide enough heat input for different hydrogen production rates. Two types of fluids, which are helium gas and molten CuCl, are investigated to transfer heat from the jacket side to the process side of the oxygen reactor. In the analysis, the Cu-Cl cycle is assumed to be driven by a nuclear reactor where two types of nuclear reactors are examined as the heat source to the oxygen reactor. These types are the CANDU Super Critical Water Reactor (CANDU-SCWR) and High Temperature Gas Reactor (HTGR). In this paper, it was found that the dominant contribution to the thermal resistance of the jacketed oxygen reactor system was from the reactor wall, where heat transfer occurred by conduction only. This contribution is about 80% of the total thermal resistance. It was also shown that a better heat transfer rate is required for SCWR than that for HTGR. Moreover, from the study of the fluid types that can be used in the service side, it was recommended to use helium gas instead of molten CuCl as a heating fluid in the jacket. Finally, it was found that the size of the oxygen reactor must be specified from the heat balance studies rather than material balance.

Keywords**:** Cu-Cl cycle; hydrogen production; oxygen; clean energy; heat transfer; Spiral Baffled Jacket

1. Introduction

Hydrogen as a clean energy carrier is frequently identified as a major solution to the environmental problem of greenhouse gases resulting from worldwide over dependence on fossil fuels. It is widely believed that hydrogen will be a significant contributing factor to sustainable energy supply in the future, since hydrogen reduces pollution of the atmosphere that contributes to climate change by reducing greenhouse gas emissions. Despite the exponentially growing need for hydrogen, the key challenge facing the hydrogen economy is the lack of sustainable production of hydrogen (without dependence on fossil fuels) in large capacities at lower costs than existing technologies. Nuclear energy offers some potential as one of the sources for large scale of sustainable production of hydrogen.

Thermochemical cycles are the promising alternatives that could be linked with nuclear reactors to thermally decompose water into oxygen and hydrogen, through a series of intermediate reactions. Copper-chlorine (Cu-Cl) cycle is identified by the Argonne National Laboratories (ANL) as one of the most promising lower temperature cycles [1]. This cycle consists of four reactions, three thermal and one electrochemical. The four reaction steps of the Cu-Cl cycle are:

$4CuCl\ (aq) \rightarrow 2CuCl_2\ (aq) + 2Cu\ (s)$, electrolytic process at 25°C step (1)

$2Cu(s) + 2HCl\ (g) \rightarrow 2\ CuCl\ (l) + H_2\ (g)$, hydro-production at 450°C step (2)

$2CuCl_2(s) + H_2O\ (g) \leftrightarrow Cu_2OCl_2(s) + 2HCl\ (g)$, hydrolysis at 375°C step (3)

$Cu_2OCl_2(s) \rightarrow 2CuCl\ (l) + \frac{1}{2} O_2\ (g)$, thermolysis at 550°C step (4)

In the oxygen production step of the Cu-Cl cycle (step 4), an intermediate compound, solid copper oxychloride (Cu_2OCl_2), is decomposed into oxygen gas and molten cuprous chloride (CuCl). The solid feed of anhydrous solid Cu_2OCl_2 is supplied to the oxygen production reactor from the $CuCl_2$ hydrolysis reaction (step 3) that operates at a temperature range of 350–450^{o}C. Gas species leaving the oxygen reactor include oxygen gas (which is evolved over a range a temperature range of 450 to 530^{o}C) and potentially impurities of products from side reactions such as CuCl vapor, chlorine gas, HCl gas (trace amount) and H_2O vapour (trace amount). The substances exiting the reactor are molten CuCl and reactant particles entrained by the flow of molten CuCl. In the oxygen reactor, the decomposition of Cu_2OCl_2 to oxygen and molten CuCl is an endothermic reaction requiring a reaction heat of 129.2 kJ/mol and a temperature of 530^{o}C, which is the highest temperature in the Cu-Cl cycle [2]. Thus, heat must be added to raise and maintain the temperature of the bulk inside the reactor.

Thermochemical properties of copper oxychloride have been examined by Ikeda and Kaye [3] and more recently by Trevani et al. [4]. Since copper oxychloride is not commercially available, methods of synthesis were developed in these two studies. The method adopted by Ikeda and Kaye [3] involved the use of stoichiometric amounts of CuO and $CuCl_2$. Lewis et al. [5], described briefly the experimental status of each of the Cu-Cl reactions. They investigated the evolution of oxygen when the Cu_2Cl_2O was heated to 530°C. They further calculated that the total amount of oxygen recovered was after 25 minutes. Zamfirescu et al. [2] examined the relevant thermo physical properties of compounds of copper that are used in thermochemical water splitting cycles. They identified the available experimental data for properties of copper compounds relevant to the Cu–Cl cycle analysis and design (Cu_2OCl_2, CuO, $CuCl_2$ and CuCl). They also developed new regression formulae to correlate the properties, which include: specific heat, enthalpy, entropy, Gibbs free energy, density, formation enthalpy and free energy. The properties were evaluated at 1 bar and a range of temperatures from ambient to 675–1000K, which are consistent with the operating conditions of the cycle. Marin provided new experimental and theoretical reference for the scale-up of a CuO*$CuCl_2$ decomposition reactor with consideration of the impact on the yield of the thermochemical copper-chlorine cycle for the generation of hydrogen [6].

Abdulrahman et al. have examined the scale-up feasibility of the oxygen reactor from the perspectives of the optimum size and number of oxygen reactors for different oxygen and hydrogen production rates. They specifically analysed the factors contributing to the oxygen reactor size. It was shown that the reactor size is significantly influenced by residence times, hydrogen production rate, mass and heat transfer [7-8]. Abdulrahman has investigated the scaleup analyses of the oxygen reactor from the perspective of indirect heat transfer using a half pipe jacketed reactor [9-12] and a helical tube inside the reactor [13]. He has concluded that the size of the reactor calculated from the perspective of heat balances is more than that calculated from the perspective of material balances. Different experiments have been performed to examine the hydrodynamics and direct contact heat transfer in the oxygen reactor [14-19]. In the experiments, empirical equations have been formulated for the gas holdup and the direct contact heat transfer coefficient in the oxygen reactor. CFD simulations have been created to examine the hydrodynamics and heat transfer for the oxygen slurry bubble column reactor using two dimensional Eulerian-Eulerian approach [20-24].

In this paper, the heat balance of the oxygen reactor in the Cu-Cl cycle is investigated analytically for different hydrogen production rates using a spiral baffled jacketed reactor. The thermal resistance of each section of the oxygen reactor system is investigated to examine the effect of each section on the heat balance. The heat balance of the oxygen reactor system is studied for Continuous Stirred Tank Reactor (CSTR) type that is heated by using a spiral baffled jacket. Two types of heat sources are studied which are Super Critical Water Reactor (SCWR) and High Temperature Gas Reactor (HTGR). Moreover, the type of the working fluid in the service side of the oxygen reactor system is examined for two types of fluids which are helium gas and CuCl molten salt, and a comparison between both fluids is performed.

2. Thermal Resistances

The continuous stirred-tank reactor (CSTR) is usually used for multiphase reactions that have fairly high reaction rates. Reactant streams are continuously fed into the vessel, and product streams are withdrawn. In CSTR, heating is achieved by a number of different mechanisms. The most common one involves the use of a jacket surrounding the vessel.

In a realistic continuous situation, where the reactor contents are at constant temperature, but with different service side inlet and outlet temperatures, the heat flow equation can be expressed by:

$$\dot{Q} = U\, A_s\, \Delta T_{lm} \tag{1}$$

where ΔT_{lm} is the log mean temperature difference between the bulk temperature of the reactor contents (cold temperature), T_c, and the temperature in the service side, T_H. Since the inside reactor temperature is assumed constant (T_c=530 ^{o}C), there is no effect of heat transfer configuration (parallel or counter flow) in the equation of ΔT_{lm} and can be written as:

$$\Delta T_{lm} = \frac{T_{H_{in}} - T_{H_{out}}}{ln\left(\frac{T_{H_{in}} - T_c}{T_{H_{out}} - T_c}\right)} \tag{2}$$

The methodology of calculations depends on the comparison of thermal resistances of each section in the oxygen reactor with the calculated total thermal resistance of the reactor system (R_t).

For a hydrogen production rate of 1 kg/day, the total amount of heat required in the oxygen reactor can be calculated as follows;

$$\dot{Q} = \Delta H_r\, \dot{\xi} + \dot{n} \int_{375}^{530} Cp_{\mathrm{Cu_2OCl_2}}\, dT = 870 \text{ W} \tag{3}$$

where $\Delta H_r = 129.162$ kJ/mol, $\dot{\xi} = 0.5$ kmol/day, $\dot{n}_{\mathrm{Cu_2OCl_2}} = 0.5$ kmol/day, $Cp_{\mathrm{Cu_2OCl_2}} = 134$ J/mol.K [2]. The limits of the integral are from 375^{o}C, which is the temperature of the fed solid, to 530^{o}C, which is the temperature of the decomposition process. For a hydrogen production rate of 100 ton/day, $\dot{n}_{\mathrm{Cu_2OCl_2}}$ is 50000 kmol/day and $\dot{Q}$ will be 87 MW.

For a high temperature gas reactor (HTGR), the nuclear reactor exit temperature is about 1000^{o}C. The inlet temperature of the heating fluid in the jacket (same as the exit temperature of the intermediate heat exchanger (IHE)) is about 900^{o}C [25]. The exit temperature from the jacket is assumed to be 540^{o}C (because the decomposition temperature is 530^{o}C). For a hydrogen production rate of 100 ton/day and number of reactors *N*, the total thermal resistance of the HTGR can be calculated as follows;

$$R_{HTGR} = \frac{1}{UA_s} = \frac{\Delta T_{lm}}{\dot{Q}} = 1.15 \times 10^{-6}\, N \quad \text{K/W} \tag{4}$$

For CANDU supercritical water reactor (CANDU-SCWR), where the nuclear reactor exit temperature is about 625^{o}C [26-27] and the inlet and outlet jacket temperatures are about 600^{o}C and 540^{o}C respectively, the total thermal resistance is $R_{SCWR} = 3.55 \times 10^{-7}\, N$ K/W for a hydrogen production rate of 100 ton/day.

3. Heat Transfer Analysis

The resistance to the heat transfer is a composite of the resistances through the various sections indicated in Fig. 1. Using the classical film theory and heat conduction through composite layers, the total thermal resistance (R_t) can be expressed as;

$$R_t = R_P + R_{FP} + R_{\mathrm{W}} + R_S + R_{FS} = \frac{1}{h_{\mathrm{P}}\, \pi\, D_{\mathrm{P}}\, H_R} + \frac{f_P}{\pi\, D_{\mathrm{P}}\, H_R} + \frac{\ln\left(\frac{D_{\mathrm{S}}}{D_{\mathrm{P}}}\right)}{2\, \pi\, k_{\mathrm{w}}\, H_R} + \frac{1}{h_{\mathrm{S}}\, \pi\, D_{\mathrm{S}}\, H_R} + \frac{f_{\mathrm{S}}}{\pi\, D_{\mathrm{S}}\, H_R} \tag{5}$$

The largest thermal resistance in Eq. (5) dominates the value of the overall heat transfer coefficient.

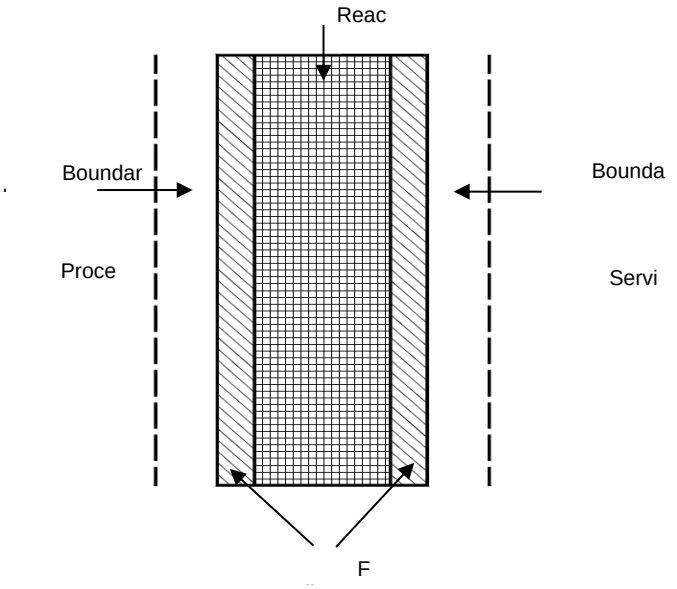

Fig. 1 Thermal resistances through the reactor wall sections.

3.1. Heat transfer through reactor wall

The stainless steels are the most frequently used corrosion resistant materials in the chemical industry. Types 321, 347 and 348 stainless steels are advantageous for high temperature service (such as in the oxygen reactor) because of their good mechanical properties. They continue to be employed for prolonged service in the 427°C to 816°C temperature range. The physical properties of Types 321, 347 and 348 are quite similar and, for all practical purposes, may be considered to be the same [28].

The ASME Code provides formulas that relate the wall thickness to the diameter, pressure, allowable stress, and weld efficiency. Since they are theoretically sound only for relatively thin shells, some restrictions are placed on their application. For cylindrical shell under internal pressure, the thickness in inches units is;

$$t = \frac{PR_R}{SE - 0.6P} + t_c \qquad conditions: \quad t \leq 0.25D_R, \quad P \leq 0.385\,SE \tag{6}$$

where t_c is the corrosion allowance in inches, R_R is the outside radius of the cylindrical shell in inches and S is the maximum allowable working stress in psi. P is the total pressure which is the sum of the static pressure and operating pressure of the oxygen reactor. The value of the joint efficiency, E, is between 0.6 and 1 [12]. In order to allow for possible surges in operation, it is customary to raise the maximum operating pressure by 10% or 0.69-1.7 bar over the maximum operation pressure, whichever is greater. The maximum operating pressure in turn may be taken as 1.7 bar greater than the normal [29].

3.2. Heat transfer through spiral baffled jacket

The cross section of a spiral baffled jacket is shown in Fig. 2. The spacing between the jacket and reactor wall depends on the size of the reactor, however, it ranges from 50 mm for small reactors to 300 mm for larger reactors [30]. In heat transfer applications, this jacket is considered a special spiral baffling case of a helical coil if certain factors are used for calculating outside film coefficients. The leakage around spiral baffles is considerable, amounting to 35–50% of the total mass flow rate. Due to the extensive leakage, the effective mass flow rate $\dot{m}'$ in the jacket is usually taken as 60% of the actual flow rate $\dot{m}$ to get a conservative film coefficient [30].

$$\dot{m}' \approx 0.6\,\dot{m} = 0.6\,\frac{\dot{Q}}{N\,C_p\,(T_{Hout} - T_{Hin})} \tag{7}$$

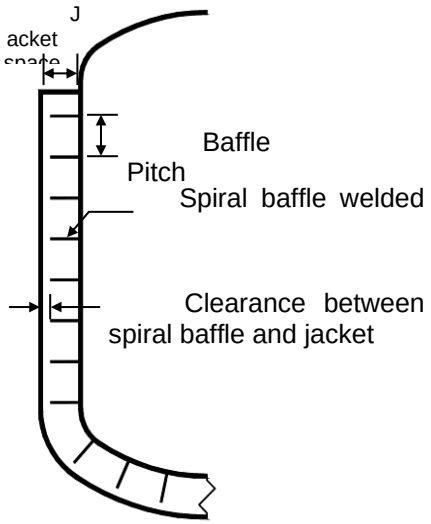

Fig. 2 Cross section of spiral baffled jacket.

where T_{in} and T_{out} are the jacket inlet and outlet temperature respectively.

The velocity of the flow in the jacket can be calculated from the effective mass flow rate by;

$$u = \frac{\dot{m}'}{\rho\,A} \tag{8}$$

where A is the spiral baffled jacket cross sectional area and ρ is the density of the service side fluid (heating fluid).

The pitch of the spiral baffled jacket can be calculated from;

$$p = \frac{A}{w} \tag{9}$$

where w is the width of the spiral baffled jacket.

The number of coils of the spiral baffled jacket can be calculated from;

$$n = \frac{H_R}{p} \tag{10}$$

where H_R is the height of the reactor.

The equivalent heat transfer diameter for the spiral baffled jacket is [30];

$$D_e = 4\,w \tag{11}$$

At a given Reynolds number, heat transfer coefficients of coils, particularly with turbulent flow, are higher than those of long, straight pipes, due to friction. This also applies to flow through a spiral baffled jacket. The equation of heat transfer should be multiplied by a turbulent flow correction factor, involving the equivalent diameter and the diameter of the spiral coil. This correction factor is equal to $\{1 + 3.5(D_e/D_c)\}$, where D_e is the equivalent heat transfer diameter for the spiral baffled jacket, which is calculated from [30]: $D_e = 4\,w$, and D_c is defined as the centerline diameter of the jacket passage.

At $Re > 10{,}000$ the Sieder-Tate equation for straight pipe can be used to calculate the outside film coefficient [30];

$$Nu = 0.027\,Re^{0.8}\,Pr^{0.33}\left(\frac{\mu_b}{\mu_w}\right)^{0.14}\left\{1 + 3.5\left(\frac{D_e}{D_c}\right)\right\} \tag{12}$$

where D_c is defined as the centerline diameter of the jacket passage and is calculated as;

$$D_c = D_{ji} + \frac{D_{j0} - D_{ji}}{2} \tag{13}$$

where D_{ji} and D_{j0} are the inlet and outlet jacket diameter respectively.

At $Re < 2{,}100$, the following equation can be used [30];

$$Nu = 1.86\,Re^{0.33}\,Pr^{0.33}\left(\frac{\mu_b}{\mu_w}\right)^{0.14}\left(\frac{D_e}{L}\right)^{0.33} \tag{14}$$

where L is the length of the spiral baffled jacket.

For $2{,}100 < Re < 10{,}000$, above equations can be used depending on the value of Re [30].

3.3. Process side heat transfer

Oxygen reactor is a multiphase reactor that contains solid particles (Cu_2OCl_2), molten salt (CuCl) and oxygen gas (O_2). In the study of indirect heat transfer, the presence of oxygen gas is neglected, because it is assumed that the oxygen gas will leave the reactor immediately after it is formed. The presence of solid particles will affect the viscosity of the molten salt. Since the density of the Cu_2OCl_2 solid (4080 kg/m^3) has a value near to that of the CuCl molten salt (3692 kg/m^3), it is assumed that solid particles and molten salt are well mixed and form homogeneous slurry. This well mixed homogeneous slurry will lead to a more uniform temperature profile inside the oxygen reactor, that's why the temperature profile is assumed to be constant and equal to 530°C. Thermo physical properties are calculated for the slurry mixture at 530°C.

The dynamic viscosity of slurry can be described as relative to the viscosity of the liquid phase;

$$\mu_{SLR} = \mu_r\,\mu_L \tag{15}$$

where μ_r is the relative dynamic viscosity (dimensionless), μ_L is the dynamic viscosity of the liquid (CuCl molten salt).

Depending on the size and concentration of the solid particles, several models exist to describe the relative viscosity as a function of volume fraction $\emptyset$ of solid particles.

$$\emptyset = \frac{V_S}{V_{SLR}} \tag{16}$$

where V_S and V_{SLR} are the volumes of solid particles and slurry respectively.

In the case of extremely low concentrations of fine particles, Einstein's equation [31] may be used;

$$\mu_r = 1 + 2.5\,\emptyset \tag{17}$$

In the case of higher concentrations, a modified equation was proposed by Guth and Simba [32], which considers interaction between the solid particles;

$$\mu_r = 1 + 2.5\,\emptyset + 14.1\,\emptyset^2 \tag{18}$$

Other thermo physical properties of the slurry mixture can be calculated from the volume percent of the solid and molten salt. For example, the average density of the slurry can be calculated as follows;

$$\rho_{SLR} = \rho_S\,\emptyset_S + \rho_L\,(1 - \emptyset_S) \tag{19}$$

where ρ_S and ρ_L are the densities of solid and liquid respectively.

The average specific heat of the slurry is;

$$Cp_{SLR} = \frac{\rho_S\,Cp_S\,\emptyset_S + \rho_L\,Cp_L\,(1 - \emptyset_S)}{\rho_{SLR}} \tag{20}$$

where Cp_S and Cp_L are the specific heats of the solid and liquid respectively.

A first order estimate of the effective thermal conductivity of a fluid filled porous media can be made by simply accounting for the volume fraction of each substance, giving the resulting relation based on the porosity and the thermal conductivity of each substance [32]. Hence, the effective thermal conductivity of the slurry is calculated from;

$$k_{SLR} = k_S\,\emptyset_S + k_L\,(1 - \emptyset_S) \tag{21}$$

where k_S and k_L are the thermal conductivities of the solid and liquid respectively.

For an agitated reactor, the inside film heat transfer coefficient (h_P) can be calculated from the following Nusselt number correlation [30];

$$Nu_D = CRe^a\,Pr^b\,\left(\frac{\mu}{\mu_w}\right)^c \tag{22}$$

where, C is constant, Re = Reynolds number $= \left(\frac{N_A\,D_A^2\,\rho}{\mu_b}\right)$ and the agitator diameter $D_A = D_R/3$

The values of constant C and the indices a, b and c depend on the type of agitator, the use of baffles, and whether the transfer is to the vessel wall or to coils. An agitator is selected on the basis of material properties and the processing required. The heat transfer forms part of a process operation such as suspending or decomposing solid particles and dispersing the oxygen gas in the molten salt. Several methods for selecting an agitator are available [34-35]. Penny showed one method based on liquid viscosity and vessel volume [36]. According to the Penny's graph and the specifications of oxygen reactor contents and size, the type of the impeller that can be used is a propeller with 420 rpm. For baffled reactor, three blades propeller and transfer to reactor wall, the Nusselt number equation is [30];

$$Nu_D = 0.64Re^{0.67}\,Pr^{0.33}\,\left(\frac{\mu_b}{\mu_w}\right)^{0.14} \qquad (Re > 5000) \tag{23}$$

3.4. Fouling resistance

An important part of the specification for the oxygen reactor is the assignment of fouling effects. A recommended way to provide an allowance for fouling, is the use of individual fouling resistance values R_{fP} and R_{fS}, for the two sides of the oxygen reactor as used in Eq. (5). R_{fP} is the fouling resistance that occurs on the internal surface of the reactor (process side) as a result of deposits that accumulate from the reactor contents. R_{fS} is the fouling resistance on the service side of the reactor (like jacket). For helium gas heating fluid, R_{fS} is expected to be negligible since there should be no build-up associated with clean dry helium. Values of the fouling resistances are specified which are intended to reflect the values at the point in time just before the exchanger is to be cleaned. Fouling of heat exchange surfaces can cause a dramatic reduction in the performance of the reactor because of the relatively low thermal conductivity of the fouling material.

There are different approaches to provide an allowance for anticipated fouling in the design of oxygen reactor. In all, the result is to provide added heat transfer surface. This generally means that the reactor is oversized for clean operation and barely adequate for conditions just before it should be cleaned.

4. Type of Working Fluid in the Service Side of Oxygen Reactor

Two types of fluids are highly recommended as working fluid in the oxygen reactor; CuCl molten salt and high-pressure helium gas (He). Helium gas is recommended amongst the other noble gases because of its chemical inertness and the relatively good transport properties [37-39].

There are substantial differences between molten salts and high-pressure helium that must be considered in selecting the working fluid as a heating medium in the oxygen reactor. These key differences are thermal performance, materials compatibility, and safety.

4.1. Thermal Performance

The thermo-physical properties for high-pressure helium and CuCl molten salt are summarized in Table 1.

Table 1 Comparison of thermo-physical properties of helium and CuCl molten salt at an average temperature of 750°C

Material	Molten Salt (CuCl) [2]	Helium (7.5 MPa)	Helium (2 MPa)
$T_{melting}$ (^oC)	430	-	-
$T_{boiling}$ (^oC)	1490	-	-
ρ (kg/m^3)	3692	3.5	0.939
C_p ($kJ/kg.^oC$)	0.66	5.2	5.2
$\rho\ C_p$ ($kJ/m^3.^oC$)	2450	18.2	4.883
k ($W/m.^oC$)	0.23	0.37	0.3687
$\mu \times 10^5$ ($pa.s$)	260	4.7	4.7
$\nu \times 10^6$ (m^2/s)	0.7	13.4	50
Pr	4.29	0.66	0.6624

From Table 1, it can be seen that the volumetric heat capacity, $\rho\ C_p$, of molten salt is over two orders of magnitude greater than that of high-pressure helium. The much higher $\rho\ C_p$ of molten salts, compared to high-pressure helium, has a significant effect upon the relative heat transfer capability. In general, a molten salt loop uses piping of smaller diameters, and less pumping power than those required for high-pressure helium. These differences in pumping power and pipe size reduce the capital cost of the piping system, and allow the arrangement of process equipment to be optimized more easily since process heat can be delivered over larger distances easily. Also, heat transfer coefficients for molten salts are typically greater than those for helium.

4.2. Materials

Two primary aspects must be considered in selecting the high-temperature materials and heating fluid used for the oxygen reactor: corrosion and high-temperature mechanical properties (strength, creep, and fabric ability). Clean helium clearly does not have the potential to corrode loop materials, while, molten salts exhibit higher corrosion rates. The potential thermal performance advantages of molten salts suggest that the high-temperature corrosion testing with molten salts should be a priority for the oxygen reactor design.

4.3. Safety

The copper-chlorine process uses chemicals which are hazardous. The heat transfer fluid in the service side of oxygen reactor provides a stored energy source that can potentially be released rapidly, generating mechanical damage and potentially dispersing flammable or toxic chemicals. For helium gas, the stored energy comes from the high pressure of the gas, and the large volume of gas due to the large duct sizes required for transferring helium with reasonable pressure losses. For molten salts, the stored energy comes from the high temperature and high heat capacity of the liquid. This energy can be released if the molten salt mixes with a volatile liquid (e.g. water), through a well-studied phenomenon typically referred to as a "steam explosion." Molten salts, due to their much lower pumping power and small piping size, permit greater physical separation between the nuclear reactor and the hydrogen production plant. This reduces or eliminates the need for berms or other structures to provide isolation between the reactor and hydrogen plant.

5. Results and Discussion

5.1. Heat transfer calculations of the oxygen reactor system

The physical properties of the heating fluid in the service side of oxygen reactor are calculated at the mean temperature of the fluid, which is for a HTGR is 720°C and for SCWR is 570°C. Table 2 shows the physical properties of both helium and molten salt CuCl for both HTGR and SCWR.

Table 2 Physical properties of helium gas and CuCl molten salt for different mean temperatures

Nuclear Reactor	Fluid	$P\ (MPa)$	$\rho\ (\frac{kg}{m^3})$	$\mu \times 10^{-5}\ (\frac{kg}{m.s})$	$k\ (\frac{W}{m.K})$	Pr	Reference
HTGR (720°C)	**Helium**	1	0.48	4.6	0.36	0.66	[40]
SCWR (570°C)	**Helium**	1	0.48	4.13	0.32	0.66	[40]
HTGR (720°C)	**CuCl**	0.1	3692	146	0.19	5	[2]
SCWR (570°C)	**CuCl**	0.1	3692	188	0.2	6.11	[2]

For a helium gas with a pressure of 1 MPa and a temperature range of 570-720°C, the compressibility factor range is 1.001426-1.009594 [40]. This factor varies from unity by less than 1% which means that helium gas can be regarded as an ideal gas. The equation of sound for gases is;

$$c = \sqrt{\gamma RT} \tag{24}$$

where γ is an adiabatic index ($\gamma_{He} = 1.6667$) and R is the gas constant ($R_{He} = 2077\ J/Kg.K$). By using Eq. (24), the theoretical maximum speed of a helium gas (which is 1/3 of speed of sound) for a HTGR (T=720°C) is 618 m/s and for a SCWR (T=570°C) is equal to 570 m/s. In this paper, to be more conservative for getting incompressible flow, the operating

speed of the helium gas is considered to be 300 m/s in baffled jacket reactor for both HTGR and SCWR. The operating speed of the CuCl molten salt is assumed to be 3 m/s for baffled jacket. These values are within the range of molten salt nuclear reactors reported [41-42].

The physical properties of the slurry mixture inside the oxygen reactor (process side) are calculated from Eq. (15) to (21). Table 3 shows the physical properties of both the solid particles and the molten salt inside the oxygen reactor at a temperature of 530°C [2, 6].

Table 3 Physical properties of Cu_2OCl_2 solid and CuCl molten salt at a temperature of 530°C

	$C_p \ \frac{J}{Kg.K}$	$k \ \frac{W}{m.K}$	$\rho \ \frac{Kg}{m^3}$
Solid Cu_2OCl_2	623.7	0.451	4080
Molten salt CuCl	650.8	0.2	3692

5.2. Heat transfer by jacketed reactor

To calculate the thermal resistance of the reactor wall, it is necessary to know the thickness of this wall. The thickness of the reactor wall (t) is calculated from Eq. (6). The pressure, P in Eq. (6) is the design pressure of the oxygen reactor which is taken here as 1.7 bar greater than the normal total pressure. The normal total pressure is the sum of the operating pressure (P_o) that is equal to 1 bar (14.5 psi) and the static pressure (P_s). Thus the design pressure is;

$$P = P_s + P_o + 1.7\ (bar) = \rho\ g\ H_R + P_o + 1.7\ (bar) \tag{25}$$

where ρ is the density of the slurry that is calculated from Eq. (19). The size of oxygen reactor has been estimated on the basis of the hydrogen production scale, mass balance, residence time, and aspect ratio, among others. The diameter range of 3-4 m and the aspect ratio of 2 were recommended for an industrial hydrogen production scale of over 100 tons/day [7]. In this paper, the value of the reactor diameter is assumed to be 4 m and the height is 8 m.

The material of the reactor wall is assumed to be stainless steel 321 and the maximum allowable working stress (S) for this stainless steel is 3600 psi at T=649°C [43]. The value of the thermal conductivity (k_w) for stainless steel 321 in the temperature range of 20-500°C is 21.4 W/m.K [38]. For known corrosive conditions, the corrosion allowance (t_c) is 8.9 mm (0.35 in.) [44]. This value is used for the oxygen reactor because of the relative high corrosion susceptibility of CuCl molten salt. The joint efficiency E is taken as 0.8. By substituting the above values into Eq. (6), the thickness of the reactor with a diameter of 4 m and a height of 8 m will be, $t = 2.7\ in = 7\ cm$

In order to calculate the thermal resistance due to fouling in the oxygen reactor, the fouling factor must be known or estimated. According to Tubular Exchanger Manufacturers Association (TEMA), the fouling factor for molten heat transfer salts is equal to 0.000088 m^2 K/W [45]. In this paper, to be more conservative, twice of this value, 0.000176 m^2 K/W, is used to be the fouling factor for molten salt CuCl.

To calculate the thermal resistance of the jacket side, it is assumed that the thickness of the jacket for spiral baffled jacket is $D_R/15$, where D_R is the reactor diameter. Table 4 shows the values of the numbers of oxygen reactors required for each section of the oxygen reactor for different heating fluids and different nuclear reactors. Figure 3 shows a comparison of the number of reactors required between HTGR and SCWR. This comparison is for each section of the oxygen reactor system with a helium gas at a pressure of 1MPa. From Table 4 and Fig. 3, it can be seen that the maximum number of reactors required comes from the wall of the reactor. This is because of the large thickness and small conductivity of the wall material. The large diameter requires thick wall to provide enough mechanical stresses and the large height produces high static pressure inside the reactor, which in turn requires more thickness for the wall. It can be seen also that the number of oxygen reactors for SCWR are higher than that for HTGR by more than three times. This is because of the higher temperature difference between the service and process sides in the HTGR. This means that using HTGR is more efficient for producing heat to the oxygen reactor than SCWR. Figure 4 shows the total number of jacketed oxygen reactors with each nuclear reactor

for both helium gas and CuCl molten salt. From this figure, it can be seen that there is no big differences between helium gas and molten CuCl in heating the jacketed oxygen reactor.

Fig. 5 shows the comparison of number of oxygen reactors versus the hydrogen production rate between material balance and heat balances for both HTGR and SCWR for a residence time of 0.5 hr and for helium gas service fluid.

From Fig. 5, it can be seen that the numbers of reactors calculated from heat balance are 18 times higher than that calculated from material balance for HTGR and 57 times for SCWR. That means the design of oxygen reactor size is controlled mainly by the heat balance.

Table 4 Number of reactors of each section of the jacketed oxygen reactor system for different heating fluids and different nuclear reactors

Nuclear Reactor Type	**Fluid Type**	**P (MPa)**	N_P	N_{FP}	N_W	N_{FS}	$N_{S-baffle}$	$N_{total-baffle}$
HTGR	He	1	1.4	1.5	27.8	0	3.4	35
	CuCl	0.1				1.5	1.4	34
SCWR	He	1	4.9	4.9	90	0	13	113
	CuCl	0.1				4.8	4.6	110

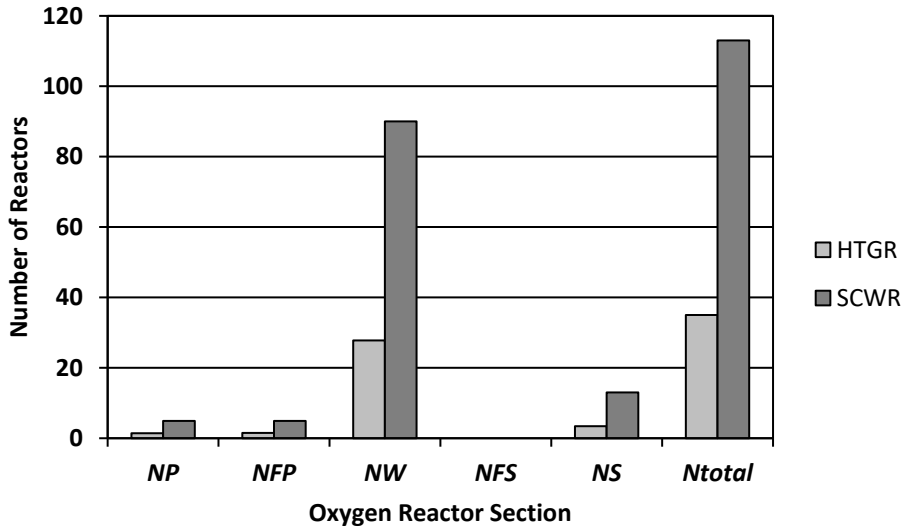

Fig. 3 Number of reactors for each section in oxygen reactor system heated by 1Mpa helium gas for both HTGR and SCWR.

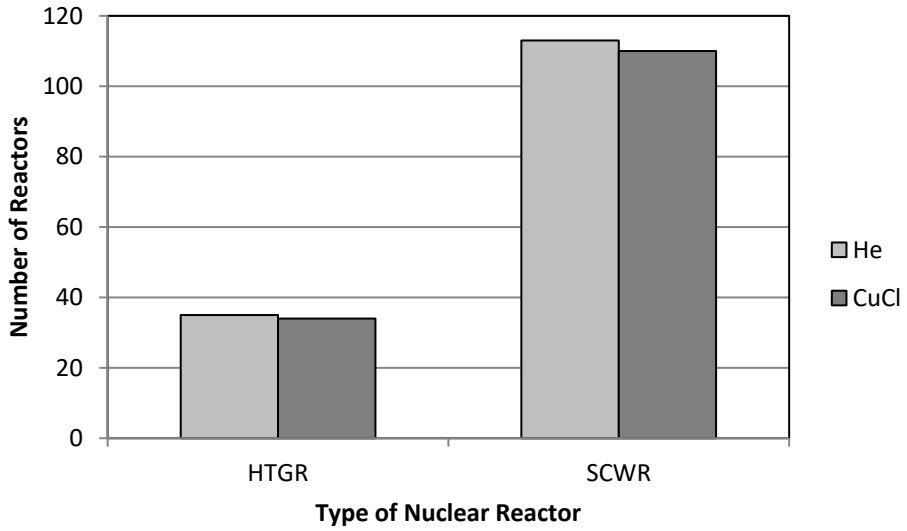

Fig. 4 Total number of oxygen reactors with each nuclear reactor for both 1MPa helium gas and CuCl molten salt.

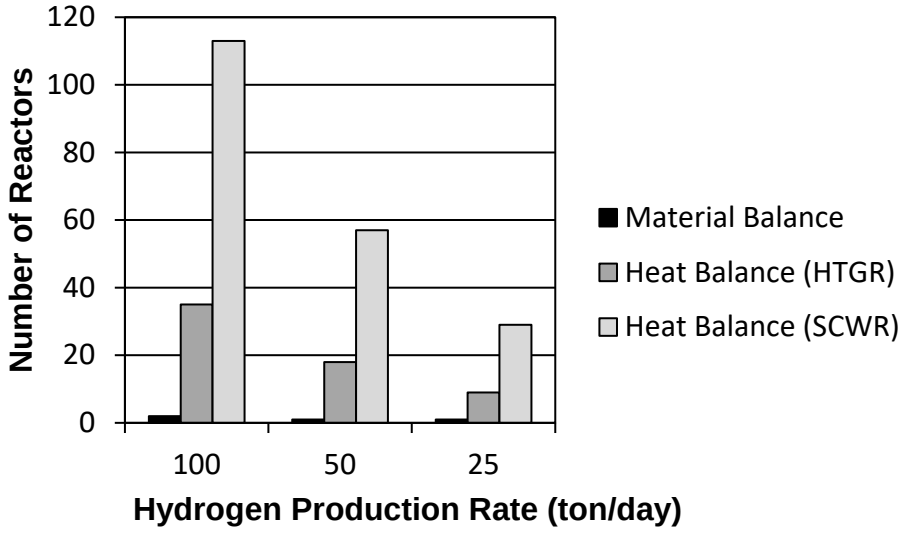

Fig. 5 Number of oxygen reactors calculated by material balance and heat balances of both HTGR and SCWR versus hydrogen production rate for a residence time of 0.5 hr.

6. Conclusions

In this paper, it can be concluded that the dominant heat transfer thermal resistance of the jacketed oxygen reactor system, is from the reactor wall which contributes in about 80% of the total thermal resistance for both types of heat sources (SCWR and HTGR). The service side contributes in about 10% and the process side and fouling in about 4% for each. The high thermal resistance of the wall is due to the large thickness and small thermal conductivity of the reactor wall.

Heat transfer calculations showed that the total thermal resistance needed for SCWR is less than that for HTGR. That means a better heat transfer rate is required for SCWR than that for HTGR. Thus, HTGR is more efficient than SCWR in

providing the required heat for the thermal decomposition process inside the oxygen reactor, because of the highest temperature difference between the service and process side in HTGR than in SCWR.

From the comparison study of the type of fluid in the service side, it is concluded that the thermal performance of the molten CuCl is better than that of helium gas which in turn is better than molten CuCl from the perspectives of material and safety aspects. By comparing the number of reactors for both fluids, it is shown that there is no significant difference between both fluids and in this case, it is recommended to use helium gas as a heating fluid in the service side of the oxygen reactor system.

From the comparison of the number of reactors obtained from material and heat balances, it is concluded that the size of the oxygen reactor is specified from the heat balance study rather than material balance.

References

[1] M. Serban, M. A. Lewis M. A. and J. K. Basco, "Kinetic Study of the Hydrogen and Oxygen Production Reactions in the Copper-Chloride Thermochemical Cycle," in *Proceedings of the AIChE, Spring National Meeting*, New Orleans, LA, 2004.

[2] Zamfirescu, I. Dincer and G. F. Naterer, "Thermophysical Properties of Copper Compounds in Copper–Chlorine Thermochemical Water Splitting Cycles," *International Journal of Hydrogen Energy*, vol. 35, pp. 4839-4852, 2010.

[3] M. Ikeda, M. H. Kaye, "Thermodynamic Properties in the Cu-Cl- O-H System," in *Proceedings of the 7th International Conference on Nuclear and Radiochemistry*, Budapest, Hungary, 2008.

[4] L. Trevani, "The copper-Cloride cycle: synthesis and characterization of copper oxychloride," in *Proceedings of the Hydrogen and Fuel Cells International Conference and Exhibition*, Vancouver, BC, May 15-18, 2011.

[5] A. Lewis, J. G. Masin and R. B. Vilim, "Development of the Low Temperature Cu-Cl Thermochemical Cycle," in *Proceedings of the International Congress on Advances in Nuclear Power Plants*, Argonne National Laboratory, Seoul, Korea, May 15-19, 2005.

[6] G. D. Marin, "Kinetics and Transport Phenomena in the Chemical Decomposition of Copper Oxychloride in the Thermochemical Cu-Cl Cycle," Ph.D. dissertation, Faculty of Engineering and Applied Sciences, University of Ontario Institute of Technology.

[7] M. W. Abdulrahman, Z. Wang and G. Naterer, "Scale-Up Analysis of Three-Phase Oxygen Reactor in the Cu-Cl Thermochemical Cycle of Hydrogen Production,". in *Proceedings of the 3rd Climate Change Technology Conference*, Concordia University, Montreal, QC, Canada, 2013.

[8] M. W. Abdulrahman, "Analysis of the thermal hydraulics of a multiphase oxygen production reactor in the Cu-Cl cycle," Ph.D. dissertation. University of Ontario Institute of Technology, Ontario, Canada.

[9] M. W. Abdulrahman, "Similitude for thermal scale-up of a multiphase thermolysis reactor in the cu-cl cycle of a hydrogen production,". *International Journal of Electrical, Computer, Energetic, Electronic and Communication Engineering*, vol. 10, no. 5, pp. 567-573, 2016.

[10] M. W. Abdulrahman, X. Wang, & G. F. Naterer, "Thermohydraulics of a Thermolysis Reactor and Heat Exchangers in the Cu-Cl Cycle of Nuclear Hydrogen Production," *(WHTC2013)*, 2013.

[11] M. W. Abdulrahman, "Heat transfer in a tubular reforming catalyst bed: Analytical modelling," in *Proceedings of the 6th International Conference of Fluid Flow, Heat and Mass Transfer*, 2019.

[12] M. W. Abdulrahman, "Exact analytical solution for two-dimensional heat transfer equation through a packed bed reactor," in *Proceedings of the 7th World Congress on Mechanical, Chemical, and Material Engineering*, 2019.

[13] M. W. Abdulrahman, "Heat Transfer Analysis of a Multiphase Oxygen Reactor Heated by a Helical Tube in the Cu-Cl Cycle of a Hydrogen Production," *International Journal of Mechanical and Mechatronics Engineering*, vol. 10, no. 6, pp. 1122-1127, 2016.

[14] M. W. Abdulrahman, "Experimental studies of direct contact heat transfer in a slurry bubble column at high gas temperature of a helium–water–alumina system," *Applied Thermal Engineering*, vol. 91, pp. 515-524, 2015.

[15] M. W. Abdulrahman, “Experimental studies of gas holdup in a slurry bubble column at high gas temperature of a helium− water− alumina system,” *Chemical Engineering Research and Design*, vol. 109, pp. 486-494, 2016.
[16] M. W. Abdulrahman, “Experimental studies of the transition velocity in a slurry bubble column at high gas temperature of a helium–water–alumina system,” *Experimental Thermal and Fluid Science*, vol. 74, pp. 404-410, 2016.
[17] M. W. Abdulrahman, “Direct contact heat transfer in the thermolysis reactor of hydrogen production Cu—Cl cycle,” U.S. Patent 10 059 586. August 28, 2018.
[18] M. W. Abdulrahman, “Material substitution of cuprous chloride molten salt and oxygen gas in the thermolysis reactor of hydrogen production Cu—Cl cycle,” U.S. Patent 10 526 201, January 7, 2020.
[19] M. W. Abdulrahman, “Simulation of Materials Used in the Multiphase Oxygen Reactor of Hydrogen Production Cu-Cl Cycle,” in *Proceedings of the 6 the International Conference of Fluid Flow, Heat and Mass Transfer (FFHMT'19),* Ottawa, Canada, 2019, pp. 123-1-123-7.
[20] M. W. Abdulrahman, “CFD simulations of direct contact volumetric heat transfer coefficient in a slurry bubble column at a high gas temperature of a helium–water–alumina system,” *Applied thermal engineering*, vol. 99, pp. 224-234, 2016.
[21] M. W. Abdulrahman, “CFD Analysis of Temperature Distributions in a Slurry Bubble Column with Direct Contact Heat Transfer,” in *Proceedings of the 3rd International Conference on Fluid Flow, Heat and Mass Transfer (FFHMT’16)*, 2016.
[22] M. W. Abdulrahman, “Effect of Solid Particles on Gas Holdup in a Slurry Bubble Column,” in *Proceedings of the 7th World Congress on Mechanical, Chemical, and Material Engineering (MCM'20),* pp. 168-1-168-10, 2020.
[23] M. W. Abdulrahman, “CFD Simulations of Gas Holdup in a Bubble Column at High Gas Temperature of a Helium-Water System,” in *Proceedings of the 7th World Congress on Mechanical, Chemical, and Material Engineering (MCM'20)*, pp. 169-1-169-10, 2020.
[24] M. W. Abdulrahman, “Temperature Profiles of a Direct Contact Heat Transfer in a Slurry Bubble Column,” *Chemical Engineering Research and Design*, vol. 182, pp. 183-193, 2022.
[25] K. Natesan, A. Moisseytsev, S. Majumdar, P. S. Shankar, *Preliminary Issues Associated with the Next Generation Nuclear Plant Intermediate Heat Exchanger Design, ANL/EXT-06/46*. Argonne National Laboratory, 2006.
[26] C. K. Chow and H. F. Khartabil, “Conceptual fuel channel designs for CANDU – SCWR,” *Nuclear Engineering and Technology, Special issue on the 3rd international symposium on SCWR,* vol. 40, no. 2, pp. 139-146, 2007.
[27] R. B. Duffey, and L. Leung, “Advanced cycle efficiency: generating 40% more power from the nuclear fuel,” *in Proceedings of the World Energy Congress (WEC)*, Montreal, Canada, 2010.
[28] Allegheny Ludlum Corporation, “Technical Data BLUE SHEET, Stainless Steels Types 321, 347 and 348,” http://www.alleghenyludlum.com, 2013.
[29] J. R. Couper, P. W. Roy, J. R. Fair and S. M. Walas, *Chemical Process Equipment Selection and Design*. Second Edition: Gulf Professional Publishing Elsevier Inc., 2005.
[30] K. Coker, *Modeling of Chemical Kinetics and Reactor Design*. Gulf Proffessional Publishing, 2001.
[31] Einstein, Ann. Physik, 19, 289, 1906.
[32] E. Guth and H. Simba, “Viscosity of Suspensions and Solutions: III Viscosity of Sphere Suspensions,” *Kolloid-Z*, vol. 74, pp. 266-75.
[33] K. Boomsma and D. Poulikakos, “On the effective thermal conductivity of a three-dimensionally structured fluid-saturated metal foam,” *International Journal of Heat and Mass Transfer,* vol. 44, pp. 827-836, 2001.
[34] S. J. Kline, *Similitude and Approximation Theory*. New York, McGraw-Hill, 1965.
[35] D. M. Himmelblau, A. Bisio, R. L. Kabel, *Scaleup of Chemical Processes*. John Wiley & Sons, 2008.

[36] W. R. Penny, “Guide to Trouble Free Mixers,” *Chem. Eng.*, vol. 77, no. 12, p. 171, 1970.

[37] P. G. Rousseau, P. G. and J. P. Van Ravenswaay, “Thermal-fluid comparison of three- and single-shaft closed loop Brayton cycle configurations for HTGR power conversion,” in *Proceedings of international congress on advances in nuclear power plants (ICAPP’03)*, Cordoba, Spain, 2003.

[38] C. Wang, R. G. Ballinger, P. W. Stahle, E. Demetri and M. Koronowski, “Design of a power conversion system for an indirect cycle, helium cooled pebble bed reactor system,” in *Proceedings of first international topical meeting on HTR technology (HTR2002)*, international atomic energy agency, Vienna, Austria, Petten, the Netherlands, 2002.

[39] J. F. Kikstra and A. H. M. Verkooijen, “Conceptual design for the energy conversion system of a nuclear gas turbine cogeneration plant,” in *Proceedings of the Institution of Mechanical Engineers, Part A: Journal of Power and Energy*. 401-411, 2000.

[40] H. Petersen, *The Properties of Helium: Density, Specific Heats, Viscosity, and Thermal Conductivity at Pressures from 1 to 100 Bar and From Room Temperature to About 1800 K. Riso Report No. 224*. Danish atomic energy commission research establishment Riso, 1970.

[41] W. R. Huntley and M. D. Silverman, “System design description of forced-convection molten-salt corrosion loops MSR-FCL-3 and MSR-FCL-4,” *Oak Ridge National Laboratory, Union Carbide Corporation for the Energy Research and Development Administration, Engineering Technology Division,* 1976.

[42] J. P. Caire and A. Roure, “Pre design of a molten salt thorium reactor loop,” *Excerpt from the Proceedings of the COMSOL Users Conference Grenoble*, 2007.

[43] E. J. Rozic, *Elevated Temperature Properties as Influenced by Nitrogen Additions to Types 304 and 316 Austenitic Stainless Steels*. ASTM International, Steel, Stainless, 1973.

[44] K. Coker, *Ludwig's Applied Process Design for Chemical and Petrochemical Plants*. Gulf Professional Publishing, 2007.

[45] J. M. Chenoweth, “Final Report of the HTRI/TEMA Joint Committee to Review the Fouling Section of the TEMA Standards,” *Heat Transfer Engineering*, vol. 11, no. 1, pp. 73-107, 1990.